


Autophagy-Related Protein ATG8 Has a Noncanonical Function for Apicoplast Inheritance in *Toxoplasma gondii*

Maude F. Lévêque,^a Laurence Berry,^a Michael J. Cipriano,^b Hoa-Mai Nguyen,^a Boris Striepen,^b  Sébastien Besteiro^a

DIMNP UMR5235 CNRS, University of Montpellier, Montpellier, France^a; Center for Tropical and Emerging Global Diseases and Department of Cellular Biology, University of Georgia, Athens, Georgia, USA^b

ABSTRACT Autophagy is a catabolic process widely conserved among eukaryotes that permits the rapid degradation of unwanted proteins and organelles through the lysosomal pathway. This mechanism involves the formation of a double-membrane structure called the autophagosome that sequesters cellular components to be degraded. To orchestrate this process, yeasts and animals rely on a conserved set of autophagy-related proteins (ATGs). Key among these factors is ATG8, a cytoplasmic protein that is recruited to nascent autophagosomal membranes upon the induction of autophagy. *Toxoplasma gondii* is a potentially harmful human pathogen in which only a subset of ATGs appears to be present. Although this eukaryotic parasite seems able to generate autophagosomes upon stresses such as nutrient starvation, the full functionality and biological relevance of a canonical autophagy pathway are as yet unclear. Intriguingly, in *T. gondii*, ATG8 localizes to the apicoplast under normal intracellular growth conditions. The apicoplast is a nonphotosynthetic plastid enclosed by four membranes resulting from a secondary endosymbiosis. Using superresolution microscopy and biochemical techniques, we show that TgATG8 localizes to the outermost membrane of this organelle. We investigated the unusual function of TgATG8 at the apicoplast by generating a conditional knockdown mutant. Depletion of TgATG8 led to rapid loss of the organelle and subsequent intracellular replication defects, indicating that the protein is essential for maintaining apicoplast homeostasis and thus for survival of the tachyzoite stage. More precisely, loss of TgATG8 led to abnormal segregation of the apicoplast into the progeny because of a loss of physical interactions of the organelle with the centrosomes.

IMPORTANCE By definition, autophagy is a catabolic process that leads to the digestion and recycling of eukaryotic cellular components. The molecular machinery of autophagy was identified mainly in model organisms such as yeasts but remains poorly characterized in phylogenetically distant apicomplexan parasites. We have uncovered an unusual function for autophagy-related protein ATG8 in *Toxoplasma gondii*: TgATG8 is crucial for normal replication of the parasite inside its host cell. Seemingly unrelated to the catabolic autophagy process, TgATG8 associates with the outer membrane of the non-photosynthetic plastid harbored by the parasite called the apicoplast, and there it plays an important role in the centrosome-driven inheritance of the organelle during cell division. This not only reveals an unexpected function for an autophagy-related protein but also sheds new light on the division process of an organelle that is vital to a group of important human and animal pathogens.

Received 16 September 2015 Accepted 29 September 2015 Published 27 October 2015

Citation Lévêque MF, Berry L, Cipriano MJ, Nguyen H-M, Striepen B, Besteiro S. 2015. Autophagy-related protein ATG8 has a noncanonical function for apicoplast inheritance in *Toxoplasma gondii*. mBio 6(6):e01446-15. doi:10.1128/mBio.01446-15.

Invited Editor Gustavo Arrizabalaga, Indiana University School of Medicine **Editor** John C. Boothroyd, Stanford University

Copyright © 2015 Lévêque et al. This is an open-access article distributed under the terms of the [Creative Commons Attribution-Noncommercial-ShareAlike 3.0 Unported license](https://creativecommons.org/licenses/by-nc-sa/4.0/), which permits unrestricted noncommercial use, distribution, and reproduction in any medium, provided the original author and source are credited.

Address correspondence to Sébastien Besteiro, sebastien.besteiro@inserm.fr.

Plasmodium falciparum and *Toxoplasma gondii* are ancient parasitic eukaryotes belonging to the phylum *Apicomplexa* and are the causative agents of malaria and toxoplasmosis, respectively. Malaria is one of the most dangerous infectious diseases around the world and is responsible for more than half a million of deaths per year (1). *T. gondii* can be found in one-third of the human population, although its infection is mostly asymptomatic. However, the parasite can cause severe disease in the case of congenital toxoplasmosis or in immunocompromised patients (2). Symptoms of the disease are directly caused by the successive lytic cycles of *T. gondii* tachyzoites, highly invasive and replicative forms capable of infecting a large variety of host cells. Following invasion, parasites proliferate through multiple division steps

within host cells, leading to their lysis and the egress of tachyzoites that are ready to invade new cells (3).

The asexual division process of these developmental forms is called endodyogeny and is characterized by the synchronous formation of two daughter cells within a mature parent cell (4). Whereas secretory organelles such as micronemes, rhoptries, and dense granules, which deliver virulence factors to the host cell during and after invasion, are synthesized *de novo* during each parasite division cycle (5), other contents are duplicated and coordinately inherited from the parent cell. These include the nucleus, the centrosomes, the Golgi apparatus, the mitochondrion, and a peculiar plastid called the apicoplast (6, 7). This organelle is the product of a secondary endosymbiosis event. As a conse-

quence, it is surrounded by four membranes, of which the outermost is thought to be analogous to the phagosomal membrane of the ancestor of *Apicomplexa* (8). Although nonphotosynthetic, the apicoplast is nevertheless essential for the survival of *Apicomplexa*, as it is involved in several key metabolic pathways (9). During the course of parasite replication, the apicoplast divides and must be segregated into each of the daughter cells for proper inheritance across generations (6, 7). The replication mechanisms of this plastid show distinct differences from typical plant chloroplasts. Shortly after apicoplast DNA replication, the organelle elongates as both ends are linked to the centrosomes of the mitotic spindle (10, 11), the machinery responsible for chromosome segregation and nuclear division (4). During budding, this association results in segregation of the organellar poles into the two growing daughters (10). At the end of this process, fission of the elongated apicoplast endows each daughter cell with a copy of the organelle (12).

Macroautophagy (simply referred to as autophagy here) is a lysosome-dependent catabolic process involved in the degradation and recycling of cellular contents, including large protein complexes and organelles. Autophagy has been extensively studied under stress conditions, such as starvation, where it recycles cellular material to provide a source of nutrients; however, it has also been characterized as a housekeeping mechanism for removing misfolded or aggregated proteins and clearing damaged organelles during normal cell growth (13). During the autophagic process, cytosolic components are sequestered within a double-membrane vesicle called the autophagosome and then delivered into a lysosomal compartment for degradation (14). This process is driven by autophagy-related (ATG) proteins, among which the ubiquitin-like protein ATG8 (known as LC3 in mammals) plays a central role (15). From a soluble cytosolic pool, ATG8 is recruited to autophagosomal membranes upon the induction of autophagy, through activation by two ubiquitination-like systems, by conjugation to the lipid phosphatidylethanolamine (PE) (16).

Proteins involved in the autophagy process are conserved across most eukaryotic phyla, including protists such as the apicomplexan parasites *P. falciparum* and *T. gondii* (17). However, it appears that the *Apicomplexa* retain only a limited set of ATG proteins, which mainly comprises the core machinery required for ATG8 conjugation to PE. While double-membrane structures decorated by ATG8 and resembling autophagosomes have been documented under acute starvation conditions (18–20), it is not clear whether these parasites are able to execute a fully functional catabolic autophagic process. Furthermore, an unusual localization has been described for ATG8 at the apicoplast during normal intracellular development in *P. falciparum* (20–25), as well as in *T. gondii* (26, 27). The function of ATG8 related to the apicoplast in these parasites remains completely unknown, but previous studies of *T. gondii* documented defects in apicoplast maintenance and reduced cell survival for mutants lacking ATG3 and ATG4, two proteins involved in the regulation of the membrane association of ATG8 (18, 26). Here, we describe an essential role for ATG8 in the inheritance of this secondary plastid during cell division. This previously unknown function of ATG8 appears to be independent of the canonical catabolic autophagy pathway. Overall, our findings provide intriguing insight into how evolution reassigns a widely conserved molecular effector to a novel task in the context of endosymbiosis and the emergence of complex eukaryotic cells.

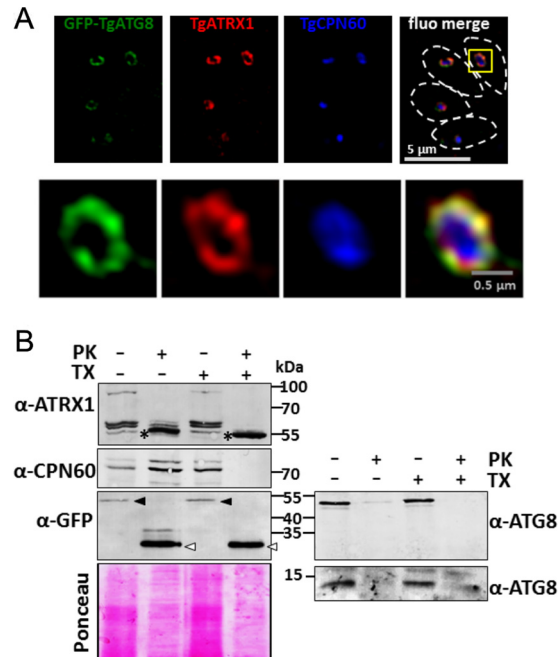


FIG 1 TgATG8 localizes to the outermost membrane of the apicoplast. (A) Structured-illumination microscopy imaging of apicoplast-localized GFP-TgATG8, together with peripheral membrane protein TgATRX1 and stromal protein TgCPN60. Parasites are delineated by dashed lines in the merged image. A magnified image of a selected organelle is shown at the bottom. (B) PK digestion assay assessing the accessibility of GFP-fused or native TgATG8, TgATRX1, and TgCPN60 to PK in the presence or absence of detergent (TX). After treatment with PK, organellar fractions were analyzed by immunoblotting and proteins were revealed with specific antibodies. Anti-GFP antibody was also used to reveal GFP-TgATG8 (black arrowheads) and proteolysis-resistant GFP (white arrowheads). The anti-TgATG8 antibody was used to reveal both GFP-fused TgATG8 and the native protein (right). The asterisks indicate a proteolysis-resistant TgATRX1 product. Ponceau red staining was used as a loading control.

RESULTS

TgATG8 localizes to the outer membrane of the apicoplast. In *Plasmodium* and *Toxoplasma*, the association of ATG8 with the apicoplast membrane is dependent on its carboxy-terminal glycine (20, 22, 26). This residue is also known to be critical for the recruitment of ATG8 to the autophagosomal membranes. The protein can be covalently linked to PE through an amide bond by a ubiquitination-like conjugation system involving, among other proteins, ATG3. Subsequently, ATG8 can be recycled from the membrane by the protease ATG4 (13). Both TgATG3 and TgATG4 have been previously localized to the cytoplasm of tachyzoites (18, 26), suggesting that TgATG8 itself, to be accessible to these proteins, should be exposed to the cytoplasmic side of the apicoplast. We used superresolution imaging of TgATG8, together with apicoplast markers, to gain a better insight into its membrane localization. Green fluorescent protein (GFP)-fused TgATG8 was found to be surrounding stromal chaperonin TgCPN60 (28), in a fashion similar to that of the peripheral membrane thioredoxin TgATRX1 (29) (Fig. 1A). Overall, this suggests that TgATG8 localizes to the periphery of the organelle.

However, even superresolution imaging cannot completely resolve individual apicoplast membranes. Thus, we next performed a proteinase K (PK) protection assay of organelle preparations to

elucidate the membrane topology of TgATG8, again with the TgCPN60 and TgATRX1 apicoplast resident proteins as controls (Fig. 1B). TgCPN60 was protected from PK and digested only in the presence of detergent, as expected for a stromal protein. In contrast, TgATRX1, which displays a complex protein profile of an 85-kDa protein and three closely migrating species between 55 and 65 kDa (29), was only partially protected from PK digestion. The addition of detergent led to the disappearance of the 85-kDa protein and partial digestion of the 55- to 65-kDa species. TgATRX1 contains a putative transmembrane domain (29); hence, it might be partially protected from PK in the absence of detergent. Immunoelectron microscopy studies have also suggested that the protein is associated with multiple peripheral membranes of the apicoplast (29), which could explain the differential susceptibilities to PK digestion. Notably, under the experimental conditions we used, incubation with PK led to an increase in a proteolysis-resistant 55-kDa TgATRX1 product, even in the presence of detergent. Importantly, with or without detergent, GFP-TgATG8 was clearly digested by PK, leading to the detection of a proteolysis-resistant 27-kDa product corresponding to a GFP monomer, as revealed with a specific antibody. Using a specific anti-TgATG8 antibody (26), we could also show that the native protein is fully accessible to PK digestion without detergent (Fig. 1B), confirming that TgATG8 is likely exposed on the cytoplasmic face of the apicoplast. Taken together, these findings suggest that TgATG8 is associated with the outermost membrane of the apicoplast.

TgATG8 is essential for *T. gondii* tachyzoite growth. Having established the localization of TgATG8 at the apicoplast outer membrane, we next wanted to elucidate its function by generating conditional TgATG8 knockdown parasites (cKd-TgATG8). To this end, we used the tetracycline-based transactivator system (30) of the TATi1-Ku80 Δ cell line (31, 32). In this cell line, we replaced the endogenous *TgATG8* promoter with an anhydrotetracycline (ATc)-regulated *TetO7Sag4* promoter by single homologous recombination. The TATi1-Ku80 Δ cell line was transfected with a linearized plasmid consisting of a dihydrofolate reductase (DHFR) resistance cassette for pyrimethamine selection and the TetO7Sag4-inducible cassette upstream of the genomic 5' coding sequence of *TgATG8* starting from the initiation codon (Fig. 2A). Following parasite transfection and drug selection, the genomic DNA of selected clones was screened by PCR to confirm successful replacement of the *TgATG8* promoter with the inducible TetO7Sag4 promoter, and one clone was chosen for subsequent analysis (Fig. 2B). We complemented this cKd-TgATG8 clone by stably integrating into the genome an additional *TgATG8* copy made to express, under the control of the tubulin promoter, a version of TgATG8 N-terminally fused with a tandem dimer of Tomato red fluorescent protein (RFP), i.e., Tomato-TgATG8. Total RNAs of the corresponding transgenic parasites, grown in the absence or presence of ATc for 3 days, were extracted for semi-quantitative reverse transcription (RT)-PCR analyses with primers specific to *TgATG8* and to β -tubulin as a control. We found that *TgATG8* transcription is effectively repressed in the conditional knockdown cell line upon the addition of ATc, while the complemented cell line exhibits a *TgATG8* transcription level similar to that of the parental cell line even under ATc regulation (Fig. 2C). This downregulation was also assessed at the protein level by Western blotting with a specific anti-TgATG8 antibody (26) (Fig. 2D). The complemented cell line was validated by the

detection of the Tomato-fused TgATG8 protein, expressed at the expected molecular mass of 62 kDa, irrespective of ATc addition. In full accordance with our RT-PCR data, TgATG8 was not detected after ATc treatment in the conditional knockdown cell line. However, we note that the endogenous protein was only faintly visible in the knockdown and complemented cell lines, even without ATc treatment, suggesting that the inducible *Sag4* promoter is weaker than the native *TgATG8* promoter (Fig. 2D). It is thus likely that, after promoter replacement, TgATG8 is expressed in residual amounts in the parasites and then completely depleted after ATc treatment.

To assess the impact of TgATG8 depletion on the *T. gondii* lytic cycle, a plaque assay was performed. The capacity of parental, mutant, and complemented parasites to produce lysis plaques in a monolayer of host cells was analyzed in the absence or continuous presence of ATc for 7 days. Depletion of TgATG8 almost completely eliminates plaque formation (Fig. 3A). Notably, cKd-TgATG8 parasites are able to produce plaques as large as those measured in the TATi1-Ku80 Δ cell line (Fig. 3B), despite the fact that TgATG8 was barely detectable by Western blotting (Fig. 2D). This suggests that, after promoter replacement, the protein is expressed in sufficient amounts to accomplish its cellular function and that its downregulation is efficiently mediated by ATc. Finally, the complemented cell line displays partial phenotypic restoration over the TgATG8-depleted cell line (Fig. 3A and B). Successful completion of the lytic cycle relies on different steps such as host invasion, parasite replication, and parasite egress from the host. We thus evaluated the ability of TgATG8-depleted parasites to invade or egress from host cells and found no particular alteration (see Fig. S1 in the supplemental material). To assess whether the defect in the lytic cycle is rather due to a replication problem, all of the cell lines were preincubated for 48 h in ATc and then allowed to infect fresh host cells for 24 h, still in the presence of ATc, prior to parasite counting. TgATG8-depleted parasites showed a delay in cell division compared to controls, as shown by the accumulation of vacuoles with mostly one or two parasites (Fig. 3C). Interestingly, an intracellular growth assay at 24 h in ATc without preincubation showed no particular defect (see Fig. S2 in the supplemental material), suggesting that replication is significantly impacted only after parasite escape from the first host cell and invasion of the second one. These data are reminiscent of the delayed-death phenotype observed in apicoplast-deprived parasites (33–35).

Depletion of TgATG8 leads to rapid loss of apicoplasts into the residual body. We thus analyzed the consequence of ATc treatment for the apicoplast by immunofluorescence assay (IFA) with an antibody against TgATRX1. We observed that TgATG8 depletion induces immediate and drastic effects on plastid maintenance, as about 60% of the cKd-TgATG8 parasites lost TgATRX1 labeling over the first day of ATc incubation. After 4 days of treatment, <5% of the parasites retained a TgATRX1-labeled organelle (Fig. 4A and B). Again, this phenotype was partially restored (30% of the remaining plastids after 4 days in ATc) in the complemented cell line (Fig. 4B). We have verified that, like native TgATG8 and GFP-fused TgATG8, at least part of the expressed Tomato-TgATG8 protein can be detected in a membrane-bound form in parasite extracts (see Fig. S3 in the supplemental material). Therefore, it is likely to be able to convey its function at the apicoplast, although the regulation of this membrane association might be less efficient. Thus, it can be speculated that the

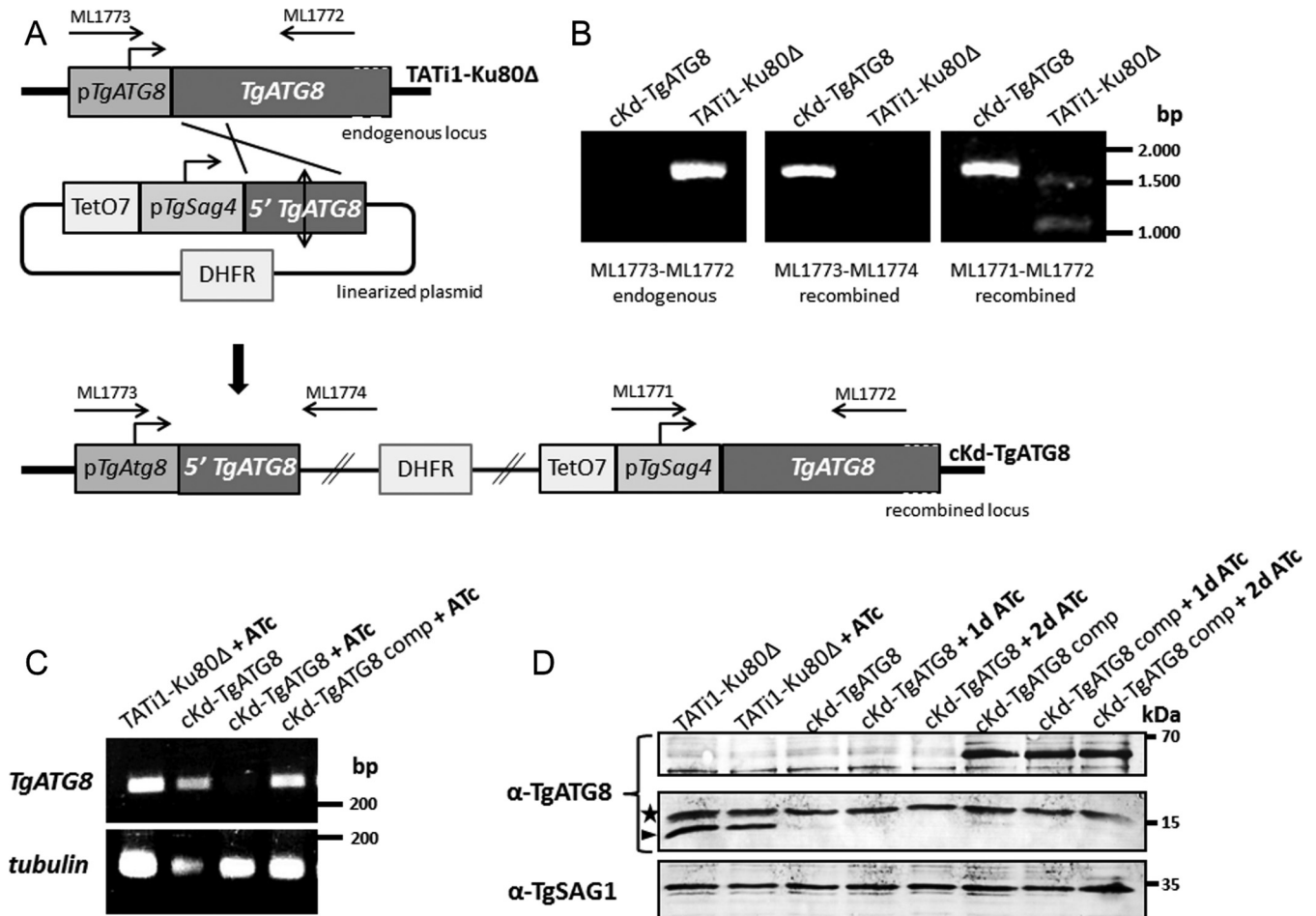


FIG 2 Genetic knockdown of *TgATG8*. (A) A *TgATG8* conditional mutant cell line was generated in a parental *TATI1-Ku80Δ* background by replacement of the endogenous promoter with an ATc-regulated promoter. Clones were obtained after pyrimethamine selection. Arrows represent the primers used to verify integration by the PCR shown in panel B. *TATI1*, transactivator; *TetO7*, *tet* operator; *DHFR*, *DHFR* selection marker; *pSag4*, *SAG4* minimal promoter. (B) Genomic DNA regions from the *TATI1-Ku80Δ* and *cKd-TgATG8* cell lines were amplified with the primer pairs depicted in panel A for PCR assay detection of the endogenous and recombined loci. (C) Semiquantitative RT-PCR analysis of *TgATG8* expression in the mutant, parental, and complemented cell lines, preceded or not by 3 days of induction with ATc to regulate expression. Specific β -tubulin primers were used as controls. (D) Western blot assay detection of *TgATG8* expression in protein extracts from *TATI1-Ku80Δ*, *cKd-TgATG8*, and complemented *cKd-TgATG8* parasites incubated in the absence or presence of ATc for up to 2 days. The anti-*TgATG8* antibody reveals the Tomato-fused *TgATG8* protein (~65 kDa) in the complemented cell line, and the endogenous *TgATG8* protein (~15 kDa, arrowhead). The star designates a probable cross-reacting signal. The anti-*TgSAG1* antibody was used as a loading control.

fairly large size of the Tomato dimer tag can somewhat prevent fully functional conjugation of *TgATG8* to the apicoplast membrane, which could explain the partial phenotypic restorations we also observed in parasite replication and plaque assays. Similar results were obtained with anti-*TgCPN60* antibody, and we also noted the loss of 4',6-diamidino-2-phenylindole (DAPI) staining of the apicoplast genome (see Fig. S4 in the supplemental material), suggesting that the entire organelle is affected by *TgATG8* depletion. During endodyogeny, organelles are coordinately packaged into two daughter cells that emerge from the mother cell, but a residual body may carry remnants of the mother cell once cell division is completed (6, 7). We observed an accumulation of apicoplasts within residual bodies in the mutant cell line (Fig. 4A) that was ~17-fold higher than that of those found in control parasites treated with ATc for 24 h (Fig. 4C). When observed by electron microscopy, the morphology of the plastids found in the residual body in the *TgATG8* mutants appeared nor-

mal with respect to their luminal contents and membranes (see Fig. S5 in the supplemental material).

Finally, to address whether other organelles were affected upon *TgATG8* depletion, we used a panel of organelle-specific markers. Secretory organelles such as micronemes, rhoptries, and dense granules or the subpellicular inner membrane complex (IMC) appeared normal (see Fig. S6 in the supplemental material). A small percentage of mutant parasites displayed fragmented mitochondria, but it was not significantly greater than that of wild-type parasites incubated for 3 days in ATc (see Fig. S6). Mutant cell lines lacking *TgATG8*-related proteins *TgATG3* and *TgATG4* had been shown to present a significant alteration of their apicoplast and their mitochondrial network (18, 26). The mitochondrial network and the apicoplast are spatially close in the parasites and also linked metabolically (9). It is thus possible that the effect on the mitochondrion observed in the *TgATG3* and *TgATG4* mutants, whose phenotypes take more time to appear after protein deple-

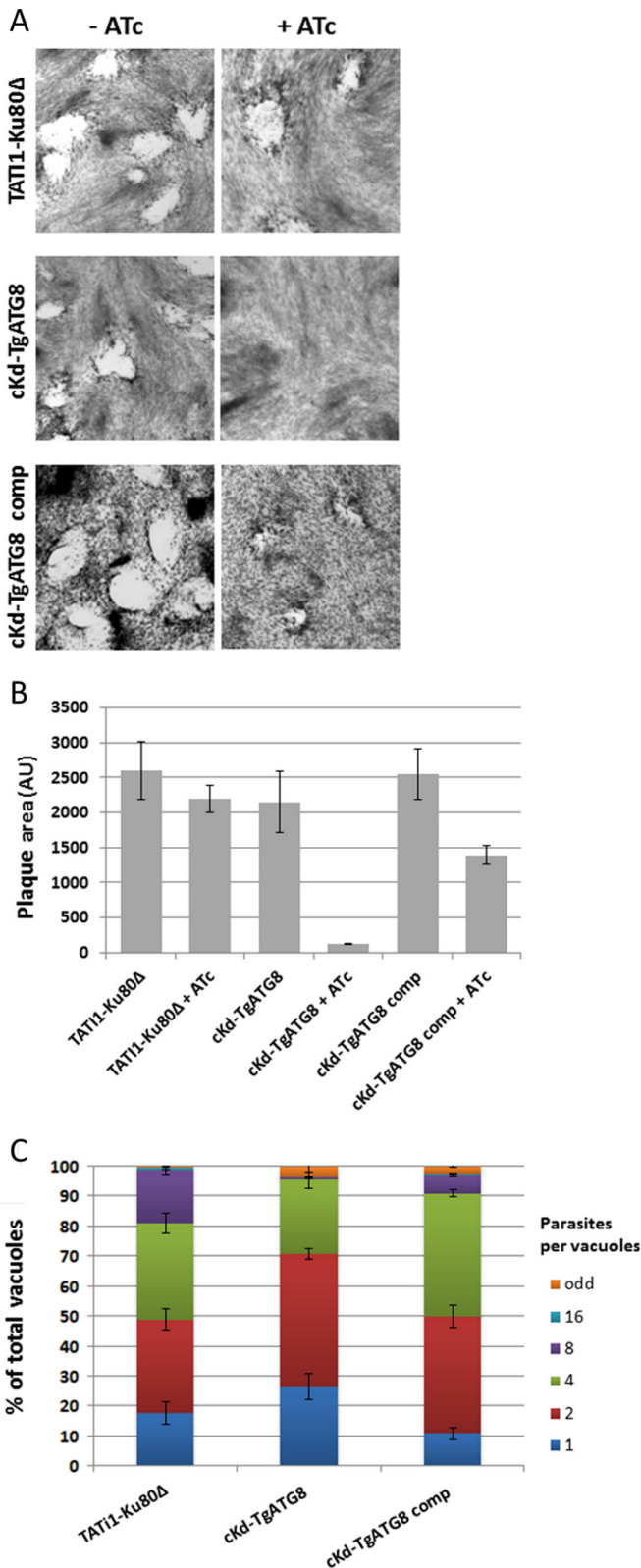


FIG 3 TgATG8-depleted tachyzoites are deficient in intracellular growth. (A) Plaque assays were carried out by infecting HFF monolayers with TATI1-Ku80Δ or cKd-TgATG8 or complemented cKd-TgATG8 parasites for 7 days with or without ATc. (B) Measurements of lysis plaque areas show a significant defect in the cKd-TgATG8 lytic cycle when parasites are incubated with ATc compared to that in the parental and complemented cell lines. AU, arbitrary (Continued)

tion, might have been a consequence of apicoplast loss rather than a direct effect. Overall, the rapid and specific loss of the apicoplast upon ATG8 downregulation suggests an important role for this protein in the maintenance of this organelle.

The apicoplast is lost during parasite division because of a segregation defect. In order to gain further insight into the mechanism of apicoplast loss, we performed IFAs with TgATRX1 and cKd-TgATG8 parasites treated for 24 h with ATc. We scored organelle loss and documented the number of divisions that had occurred by determining the number of parasites per vacuole (Fig. 5A). Plastid loss progressed with the number of parasite divisions; while vacuoles with a single parasite retained the organelle in most cases, those that had divided three or four times to form 8 or 16 daughters, respectively, showed the most dramatic loss. As all of the parasites had experienced ATc for the same amount of time, this suggested that apicoplast loss may occur during division. To assess whether the partition of the apicoplasts is affected in TgATG8-depleted tachyzoites, we investigated the subcellular localization of the remaining plastids specifically within dividing parasites (Fig. 5B). IFAs were performed with cKd-TgATG8 and control cell lines treated for 24 h with ATc, and the TgATRX1 signal was analyzed along with IMC-1, a marker that permits the visualization of nascent daughter cells (36). Interestingly, only 1% of the TgATG8-depleted dividing tachyzoites contained an apicoplast within both of their daughter cells. On the other hand, about half of the dividing parasites presented abnormal situations in which the apicoplast was still present within the mother cell or present within only one of the two growing cells. The other half of the dividing mutants had simply lost their plastids. Electron microscopic observations of dividing TgATG8-depleted parasites showed normal-looking apicoplasts that were mispositioned or, in several cases, seemed to be dragged along the extending daughter cell IMC, apparently en route to the residual body (Fig. 5C). Accumulation of intact plastids within residual bodies (Fig. 4C), as well as the loss of apicoplasts (Fig. 4B) throughout cell division (Fig. 5A), is consistent with a defect in apicoplast segregation between daughter cells (Fig. 5B and C). Taken together, these results demonstrate that TgATG8 is required for apicoplast inheritance.

TgATG8 is important for linking the apicoplast to the centrosomes during division. During the division of the apicoplast, each end of the elongated organelle remains associated with one of the duplicated centrosomes and is guided into the growing daughter (10) (Fig. 6A). With the aim of elucidating more precisely the mechanism that could prevent the proper segregation of the apicoplast into daughter cells in TgATG8-depleted parasites, we looked at the apicoplast association with centrosomes labeled with anti-TgATRX1 and anti-centrin1 antibodies, respectively (Fig. 6B). Prior to cell division, plastids in the parental cell line appear rather indistinguishable from those in TgATG8-depleted parasites. However, as organelle division progresses, while the two ends of the U-shaped apicoplast are linked

Figure Legend Continued

units. Values are the mean ± the standard error of the mean of four experiments. (C) Intracellular growth of TATI1-Ku80Δ, cKd-TgATG8, and complemented cKd-TgATG8 parasites preincubated for 48 h in ATc and allowed to invade new HFFs, still in the presence of ATc. The number of parasites per vacuole was determined 24 h after inoculation. Values are the mean ± the standard error of the mean of three independent experiments, where 200 vacuoles were counted for each condition.

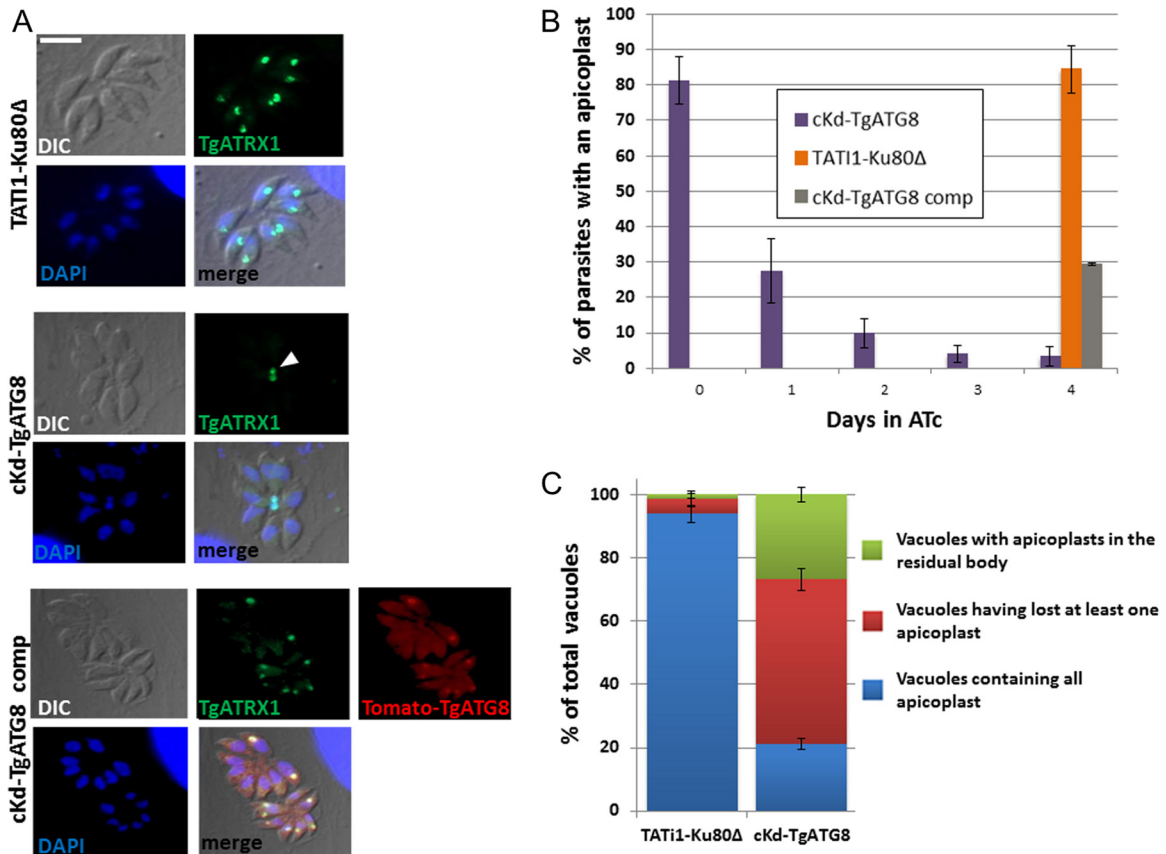


FIG 4 TgATG8-depleted tachyzoites rapidly lose apicoplasts, and remaining plastids accumulate in residual bodies. (A) Immunofluorescence assay for detection of apicoplast marker TgATRX1 in HFF monolayers infected with TATI1-Ku80 Δ , cKd-TgATG8, and complemented cKd-TgATG8 parasites treated for 4 days with ATc. Tomato-TgATG8 native fluorescence was detected with a Texas Red filter. DNA was labeled with DAPI. The arrowhead indicates apicoplasts within a residual body. Scale bar, 5 μ m. (B) Quantification of the number of apicoplasts present in the TgATG8 conditional mutant, parental, and complemented cell lines grown on HFF monolayers for 0, 1, 2, 3, or 4 days in ATc. Values are the mean \pm the standard error of the mean of three independent experiments; 200 parasites were counted for each condition. (C) Quantification of the number of vacuoles containing at least one apicoplast within the residual body or with at least one parasite having lost an apicoplast or containing all of their apicoplasts in the cKd-TgATG8 mutant and TATI1-Ku80 Δ parental cell lines grown on HFF monolayers for 24 h in ATc. Values are the mean \pm the standard error of the mean of two independent experiments, where 200 parasites were counted for each condition.

to the duplicated centrosomes and inserted into the nascent daughter cells in the control cell line, this association in the mutant is either completely or partially ablated (only one end of the organelle associates with a centrosome) (Fig. 6C). As a consequence, nonsegregated apicoplasts remain within the mother cell or are asymmetrically distributed into only one of the daughters. In complemented parasites, Tomato-TgATG8-decorated apicoplasts appeared to be normally associated with the centrosomes during division (Fig. 6D). We did not observe obvious defects in the duplication or segregation of the centrosome itself in the mutant. Centrosomes also coordinate the division of the Golgi apparatus (37), so we evaluated the centrosome association and daughter cell distribution of the Golgi marker GRASP in TgATG8-depleted parasites and found that it was unperturbed (see Fig. S7 in the supplemental material).

We sought to investigate more precisely the potential spatial and temporal regulation of TgATG8 function at the apicoplast during organelle division. When imaging the localization of GFP-TgATG8 in elongated apicoplasts, we noticed that the protein was not uniformly distributed but rather predominantly enriched at the ends of the organelles (Fig. 7A). As a consequence, GFP-

TgATG8 was located close to the centrosomes (Fig. 7B). Super-resolution imaging revealed that during division, GFP-TgATG8 caps the ends of the plastid. Importantly, TgCPN60 and TgATRX1 did not show such a polar distribution over the elongated organelle (Fig. 7C). We next used time-lapse live microscopy to study the dynamics of TgATG8 association with the apicoplast. While the GFP-TgATG8 construct is driven not by the native TgATG8 promoter but by a tubulin promoter instead, we note that the two genes show similar expression profiles across the cycle (<http://www.toxodb.org>) (38). We imaged intracellular parasites coexpressing GFP-TgATG8 and Tomato-TgIMC1 to highlight budding daughter cells. We observed a striking recruitment of GFP-TgATG8 to the apicoplast, just prior to the formation of daughter cell scaffolds (see Movie S1 in the supplemental material). Costaining of GFP-TgATG8 with the Golgi apparatus marker GRASP shows that this happens after Golgi apparatus division and thus after centrosome duplication (see Movie S2 in the supplemental material). The timing and localization of ATG8 recruitment to the centrosome-associated poles of the organelle are consistent with a specific and localized function for TgATG8 during elongation and segregation of the apicoplast (6).

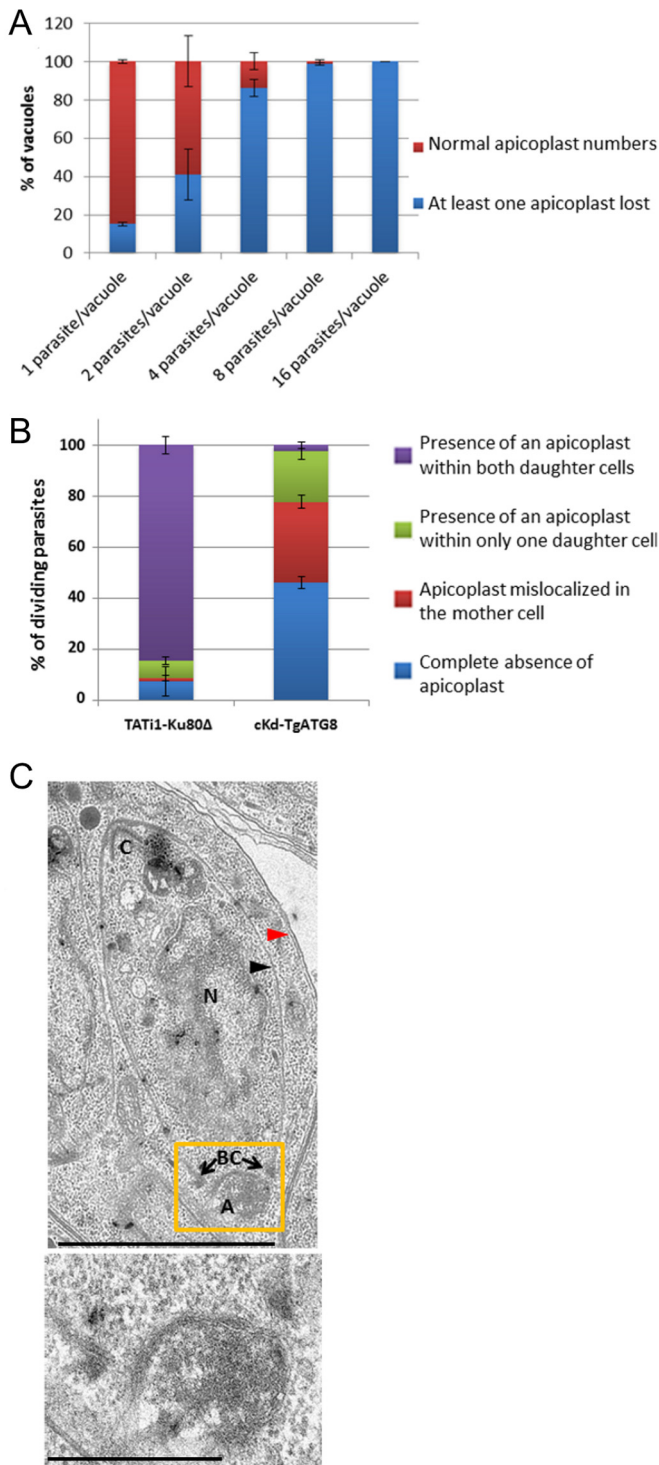


FIG 5 Contribution of TgATG8 to apicoplast inheritance. (A) Quantification of the presence of all apicoplasts or the absence of at least one in vacuoles containing 1, 2, 4, 8, or 16 TgATG8 conditional mutant tachyzoites grown on HFF monolayers for 24 h in ATc. Values are the mean \pm the standard error of the mean of two independent experiments where 100 parasites were counted for each condition. (B) Quantification of the number of TATi1-Ku80 Δ and cKd-TgATG8 dividing tachyzoites incubated for 24 h in ATc that contain no apicoplast or harbor an apicoplast within only one daughter cell or within the mother cells or with apicoplasts normally segregated within both daughters cells. Values are the mean \pm the standard error of the mean of two independent experiments, where 200 parasites were counted for each condition. (C) Elec-

(Continued)

DISCUSSION

ATG8 is a protein that plays an essential role in autophagosome biogenesis (39). To be able to perform its function at the autophagosome, it undergoes a unique ubiquitination-like conjugation, through a C-terminal glycine of the protein, to a specific phospholipid on the autophagic membrane. Although we have previously shown that TgATG8-decorated autophagosomes can be induced by stresses such as nutrient starvation in *Toxoplasma* tachyzoites, an unusual localization of ATG8 at the apicoplast during normal intracellular parasite development has also been described more recently for both *Plasmodium* (20–25) and *Toxoplasma* (26, 27). Yet, this localization and the apicoplast-related function of ATG8 remained enigmatic. We now show that TgATG8 is likely located on the outermost membrane of the organelle. The C-terminal glycine residue of apicomplexan ATG8 is important for apicoplast localization, and involvement of the ATG3 and ATG4 proteins in apicoplast homeostasis has been shown previously (18, 26). This suggests that the parasites have subverted the machinery for conjugating ATG8 to the autophagosomal membranes in a similar fashion for apicoplast binding and that this function is important for the parasite.

TgATG8 is present in both soluble and membrane-associated forms under normal parasite growth conditions (18), and native TgATG8 has been shown to localize both in the cytoplasm and with dividing apicoplasts (26). Our live-imaging experiments with GFP-tagged TgATG8 now illustrate that this association with the apicoplast membrane appears to be regulated during the cell cycle. Microarray data (38), searchable through ToxoDB ([http://www-toxoDB.org](http://www.toxoDB.org)), have revealed that although TgATG8 mRNA levels vary little during the cell cycle, its two autophagosome-conjugating partners TgATG3 and TgATG7 both seem expressed predominantly toward the end of the G₁ phase. This is consistent with an increased association of TgATG8 with the apicoplast membrane when the organelle divides. As for the recycling of the protein from the apicoplast, which seems to occur to some extent after the organelle has been segregated into daughter cells, it is likely to be mediated by cysteine protease TgATG4 (26).

Yeast ATG8 has been shown to mediate membrane tethering and hemifusion *in vitro* (15); it could thus be hypothesized that TgATG8 has a role in apicoplast membrane biogenesis during the duplication of the organelle. However, at early time points after TgATG8 depletion, we observed rather bulky or elongated apicoplasts, which had already lost their association with the centrosome, suggesting that the replication of the organelle is not particularly impacted by the loss of TgATG8. Besides, no particular morphological defect was observed by electron microscopy of the four membranes of abnormally segregated apicoplasts or organelles that were found in residual bodies. A role for TgATG8 in membrane elongation during cell division is not to be completely excluded, but the most striking phenotype we observed in the mutant was instead a loss of apicoplast association with the centrosomes during the segregation of the organelle in nascent para-

Figure Legend Continued

tron microscopy showing a mislocalized apicoplast outside a forming daughter cell in TgATG8-depleted tachyzoites grown for 24 h in ATc on HFF monolayers. Black arrowhead, daughter IMC; red arrowhead, parent IMC; C, conoid; N, nucleus. The apicoplast (A), of which a magnified view is presented at the bottom, is localized abnormally close to the basal complex (BC). Scale bars, 2 μ m (top) and 500 nm (bottom).

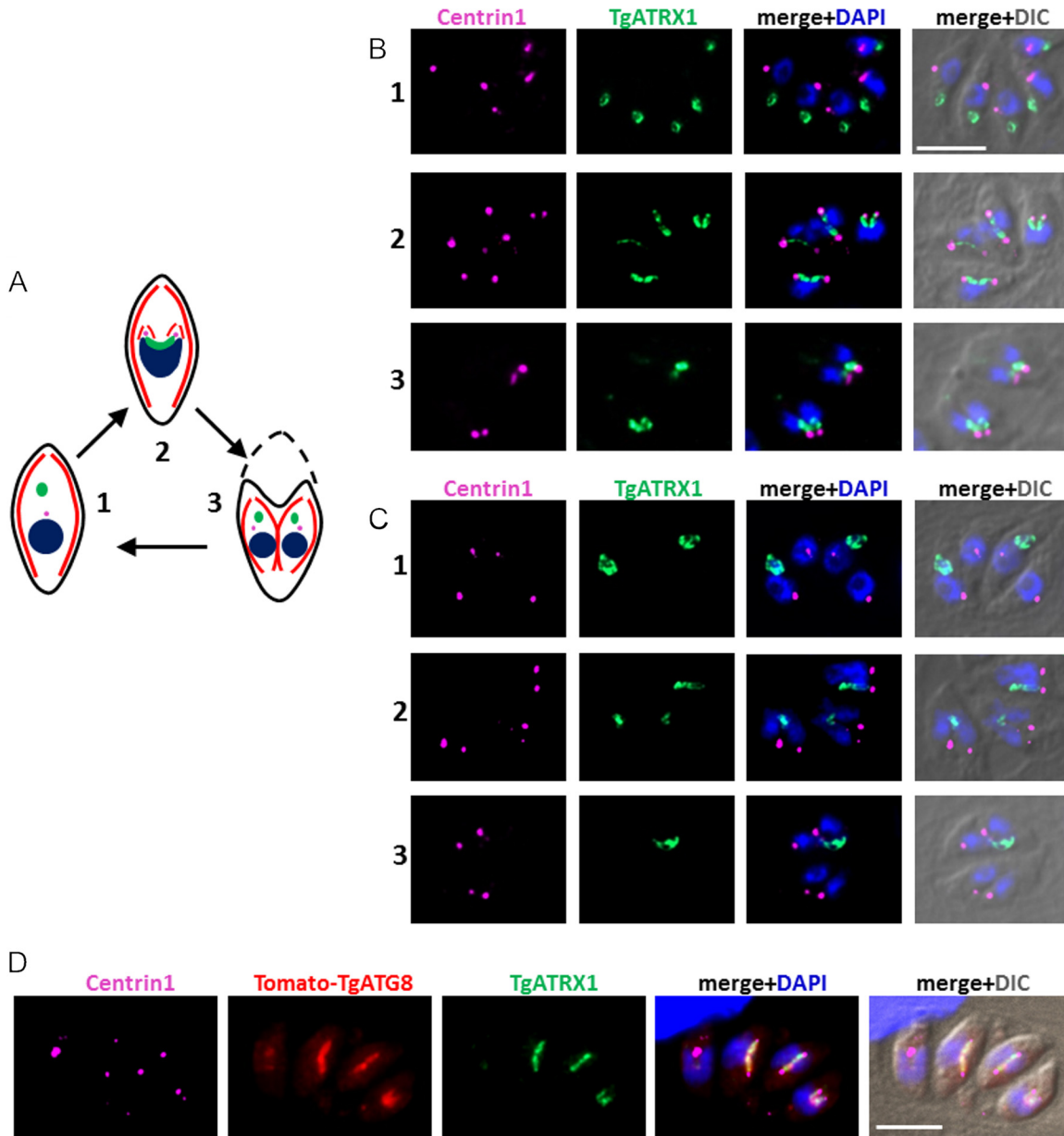


FIG 6 The ends of dividing apicoplasts are no longer linked to centrosomes in TgATG8-depleted tachyzoites. (A) Schematic summary describing apicoplast division and association with centrosomes during endodyogeny. Part 1 shows a mother cell comprising a centrosome and an ellipsoid apicoplast located apical to the nucleus prior to endodyogeny. Part 2 shows that as the nucleus divides, elongated U-shaped apicoplast are associated with the two duplicated centrosomes and inserted into the two growing daughter cells during endodyogeny. Part 3 shows that upon degeneration of the mother cell, fully assembled daughter cells incorporate its plasma membrane at the end of endodyogeny. The apicoplast is green, the nucleus is blue, the centrosome is pink, the IMC is red, and the plasma membrane is black. (B, C) Immunofluorescence analysis of HFF monolayers infected for 24 h in the presence of ATc with parental TATi1-Ku80Δ (B) and mutant cKd-TgATG8 (C) parasites. Different steps of parasite division, corresponding to those described in panel A, are shown. The apicoplast was labeled with anti-TgATR1 antibody, and centrosomes were labeled with anti-centrin1 antibody. DNA was labeled with DAPI. Scale bar, 5 μ m. (D) Immunofluorescence analysis of HFF monolayers infected for 24 h in the presence of ATc with complemented cKd-TgATG8 parasites. The apicoplast was labeled with anti-TgATR1 antibody, and centrosomes were labeled with anti-centrin1 antibody; Tomato-TgATG8 native fluorescence was detected with a Texas Red filter; DNA was labeled with DAPI. Scale bar, 5 μ m. DIC, differential interference contrast.

sites. It can thus be postulated that TgATG8 primarily plays a role in the positioning of the organelle with regard to the centrosomes or in the establishment of a link with them.

Centrosomes are one of two microtubule-organizing centers (MTOCs) found in *Toxoplasma* tachyzoites; they act as the MTOC for the spindle microtubules during parasite budding, while in

mature parasites, the polar ring associated with the apical conoid complex acts as the MTOC and site of origin of the subpellicular microtubules associated with the IMC. In mammalian cells, autophagosomes move in a microtubule- and dynein/dynactin motor complex-dependent manner (40). Ultimately, they concentrate near an MTOC, next to which lysosomes can also be found

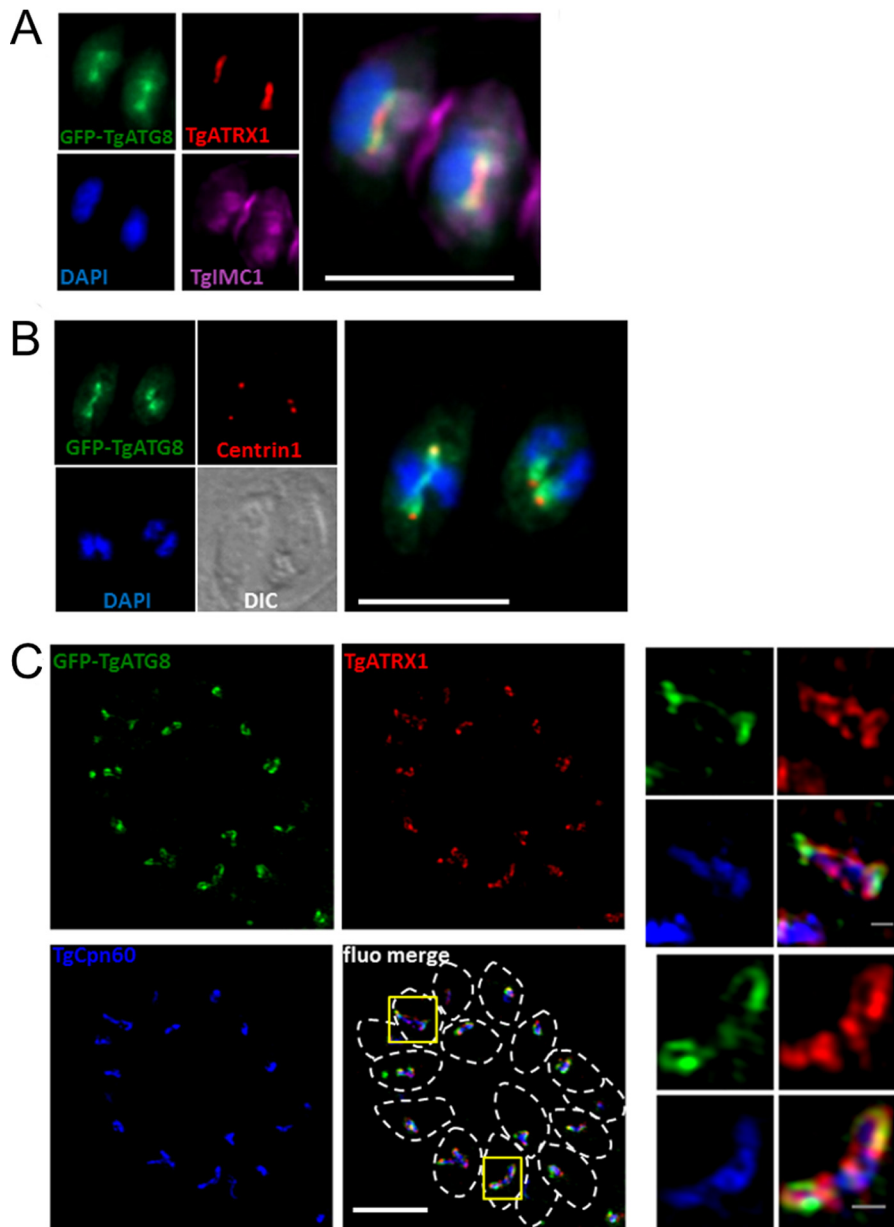


FIG 7 TgATG8 is enriched at the ends of elongating apicoplasts. (A) Dividing parasites expressing GFP-TgATG8 with the daughter cell scaffold labeled with TgIMC1 and containing elongated apicoplasts labeled with TgATRX1. DNA was stained with DAPI. A magnified merged image is displayed on the right. (B) In dividing parasites expressing GFP-TgATG8, centrosomes were labeled with anti-centrin1 antibody and DNA was labeled with DAPI. DIC, differential interference contrast. (C) Structured-illumination microscopy imaging of GFP-TgATG8 at elongated apicoplasts together with peripheral membrane protein TgATRX1 and stromal protein TgCPN60. Parasites are delineated by dashed lines in the merged image. Magnified images of selected organelles (yellow squares) are displayed on the right. Scale bars: A and B, 5 μm ; C, 5 μm (merged image) and 0.5 μm (magnified images).

(41). LC3, the mammalian ATG8 orthologue, is enriched in microtubule-containing subcellular fractions (41). More precisely, it has been shown to associate with microtubules through interaction with microtubule-associated proteins MAP1A, MAP1B, and MAP1S (42, 43). Altogether, the above data support the idea that the trafficking of stress-induced autophagosomes along microtubules and toward an MTOC could depend on LC3. Interestingly, components of the autophagic machinery, including LC3, have also been located around the basal body of mammalian cells' primary cilia (44). Thus, there is also growing evi-

dence that ATG8-like proteins could interact with MTOCs, although the molecular actors that mediate this interaction are unknown.

In *Toxoplasma*, daughter cells assemble within their parent cell in a stepwise and highly ordered process that is temporally and spatially guided by a self-organizing cytoskeleton (4). Microtubules are thus important for the coordination of nuclear division and budding (10, 45). The microtubule-associated proteins that mediate LC3 binding have no clear homolog in *Toxoplasma*; thus, it is unclear how TgATG8 could act as an intermediate between

the apicoplast and microtubules. However, the LC3/ATG8 family of proteins is known to be able to interact directly with a surprisingly large variety of protein partners through a specific amino acid recognition motif (46, 47). Thus, binding of TgATG8 to microtubules through other adapters, or even directly to another type of cytoskeleton, can be speculated. Interestingly, a recently described myosin F mutant displays quite similar defects in apicoplast positioning and segregation into daughter cells (48). The authors have suggested that myosin F would be involved in correct positioning of the centrosomes rather than directly act on apicoplast movement, but the actin-myosin-dependent movement of chloroplasts is well documented in plants (49), and this also remains a possibility. In our case, one should note that after TgATG8 depletion, centrosomes appear to be correctly duplicated and positioned, while the association with the apicoplast is already lost. We have shown that TgATG8 recruitment to the apicoplast membrane is temporally regulated, with an increased association when the organelle starts dividing. It also seems to be spatially regulated as the protein appears to cap specifically elongated organelles. Altogether, it makes TgATG8 ideally poised to drive the association between the apicoplast and the centrosomes for correct positioning and segregation of the organelle during cell division.

It is unknown if this original function of ATG8 would be conserved in other *Apicomplexa*. *Plasmodium* parasites appear to lack obvious centrioles, but they do contain spindle pole plaques that function in chromosomal division and might also serve to drive apicoplast elongation (50, 51), although this may not be true for all parasitic stages (52). Because of the clear apicoplast localization of ATG8 in *Plasmodium*, one can only speculate that its putative function in coordination of plastid division is conserved, and this deserves to be assessed experimentally.

Toxoplasma has a single *ATG8* gene, but many other eukaryotes contain multiple *ATG8* homologs, which is likely to reflect redundancy but also functional specialization (39). Although they can be described as having a general role in membrane trafficking events, these *ATG8*-like proteins have functions that clearly go beyond the sole autophagic pathway. Because of their reversible membrane association, they would be perfectly suited for a regulated general scaffolding function for organelles other than autophagosomes. The individual roles of these paralogs in autophagy are only beginning to emerge, and our findings on *Toxoplasma* may constitute a striking example of a specialized and noncanonical function for *ATG8* that emerged in an early-diverging eukaryote.

MATERIALS AND METHODS

Host cells and *T. gondii* culture. *T. gondii* tachyzoites (RH, TATI1-Ku80Δ and derived transgenic cell lines) were grown at 37°C in confluent human foreskin fibroblasts (HFFs) maintained in Dulbecco's modified Eagle's medium (DMEM; Gibco-BRL) supplemented with 5% fetal calf serum, 2 mM glutamine, and a cocktail of 100 μg/ml penicillin-streptomycin.

PK digestion assay. Parasites were lysed by sonication in homogenization buffer (250 mM sucrose, 1 mM EDTA, 10 mM morpholinopropanesulfonic acid [MOPS, pH 7.2], 2 mM dithiothreitol) and centrifuged at $1,500 \times g$ for 10 min to remove intact cells. An organellar fraction was obtained by centrifugation at $15,000 \times g$ for 30 min. The pellet was resuspended in homogenization buffer. PK (Sigma) and Triton X-100 were optionally added at 0.1 mg/ml and 0.5% (vol/vol), respectively, and the

mixture was incubated for 30 min at 4°C before analysis by SDS-PAGE and immunoblotting.

Plasmid constructions and parasite transfections. For the primers used in this study, see Table S1 in the supplemental material. Plasmid DHFR-TetO7Sag4-TgATG8 was designed to generate the cKd-TgATG8 cell line with the Tet-off system. The 5' end of *TgATG8*, starting from the initiation codon, was amplified from genomic DNA by PCR with the Phusion polymerase (New England BioLabs) and the ML1737/1738 primers. The 1.5-kbp fragment was then cloned into the DHFR-TetO7Sag4 plasmid by using BglIII/NotI (32, 53) downstream of the ATc-inducible TetO7Sag4 promoter. The DHFR cassette was used as a marker for selection of transgenic parasites. The TATI1-Ku80Δ cell line was transfected with 80 μg of the BsiWI-linearized DHFR-TetO7Sag4-TgATG8 plasmid. Transgenic parasites were selected with pyrimethamine and cloned by limiting dilution. Positive clones were verified by PCR to detect the native locus with the ML1773/1772 primers and the recombinant locus after integration with ML1773/1774 and ML1771/1772. Conditional expression of the construct generated was performed with 1 μg/ml ATc. The TgIMC1-Tomato plasmid was constructed by cloning the *TgIMC1* gene with BglIII/AvrII at the 5' end of two copies of the gene coding for the Tomato RFP and driven by flanking 5' α-tubulin and 3' DHFR genomic regions from *T. gondii*. The construct used to obtain N-terminally fused tandem dimer Tomato-TgATG8 was generated by cloning a PCR fragment obtained with primers ML971/972, corresponding to the *TgATG8* cDNA, with the SmaI/EcoRV restriction sites, at the 3' end of two copies of the gene coding for the Tomato RFP to yield the pTub-Tomato-TgATG8-CAT plasmid. A glycine 124 mutant version of Tomato-TgATG8 was generated by site-directed mutagenesis with primers ML1017 and ML1018. For the complementation strategy, the cKd-TgATG8 cell line was transfected with 40 μg of a circular pTub-Tomato-TgATG8-CAT vector and subjected to chloramphenicol selection.

Semiquantitative RT-PCR. RNAs were extracted with the NucleoSpin RNA II kit (Macherey-Nagel) from extracellular *T. gondii* tachyzoites incubated with or without ATc for 3 days. cDNAs were produced with 600 ng of total RNA per RT-PCR reaction mixture with the Superscript III first-strand synthesis kit (Invitrogen). Specific *TgATG8* ML1884/1885 primers and, as a control, β-tubulin ML841/842 primers were used for PCR with the LA Taq polymerase (TaKaRa). Twenty cycles of denaturation (10 s, 95°C), annealing (30 s, 60°C), and elongation (15 s, 68°C) were performed to detect the *TgATG8* locus.

Western blot analysis. Protein extracts from 10^7 freshly egressed tachyzoites kept with or without ATc for 1 or 2 days were separated on a 12% acrylamide gel. Endogenous and complemented TgATG8 was detected with a rabbit anti-TgATG8 (26) antibody (1/1,000). A mouse anti-SAG1 (54) antibody (1/2,000) was used for loading controls.

Plaque assay. A confluent monolayer of HFFs grown in 24-well plates was infected with freshly egressed tachyzoites and incubated with or without ATc for 7 days before the cells were fixed in cold methanol. The host cell layer was then stained with Giemsa. Images were acquired with an Olympus MVX10 macro zoom microscope equipped with an Olympus XC50 camera. Plaque area measurements were performed with AxioVision software (Zeiss). Independent experiments were conducted four times.

Egress assay. A total of 1×10^5 tachyzoites were inoculated onto HFFs, grown in a 24-well plate, washed at 2 h postinfection, and then allowed to replicate in the absence or presence of ATc for 30 h. Intracellular parasites were then incubated with DMEM containing 0.15% dimethyl sulfoxide (DMSO) or 3 μM calcium ionophore A23187 (Sigma) in DMSO for 5 min at 37°C before fixation with 4% (wt/vol) paraformaldehyde in phosphate-buffered saline (PBS) for 20 min. Percentages of egressed vacuoles were assessed by IFA with an anti-GRA3 antibody (55) to visualize the extent of vacuole lysis and an anti-SAG1 antibody (54) to identify parasite spreading. Independent experiments were conducted three times, and 250 vacuoles were counted for each condition.

Invasion assay. A total of 5×10^6 freshly egressed tachyzoites treated for 24 h with ATc were sedimented onto new HFFs for 30 min at 4°C and incubated for 5 min at 38.5°C to allow invasion. Invasion was stopped by fixation with 4% (wt/vol) paraformaldehyde in Hanks' balanced salt solution (HBSS) for 20 min and was assessed by IFA. Extracellular tachyzoites were blocked with 0.1% (wt/vol) bovine serum albumin (BSA) in HBSS and labeled with an anti-SAG1 antibody (54). Intracellular tachyzoites were identified with a rabbit anti-ROP1 antibody (1/1,000; gift from J. F. Dubremetz [unpublished data]) after permeabilization with 0.5% (wt/vol) saponin in PBS and blocking with 0.1% (wt/vol) BSA in PBS. The number of intracellular or attached parasites was scored in at least five random microscopic fields.

Intracellular growth assay. HFFs were infected with freshly egressed tachyzoites pretreated for 48 h with ATc and kept in the presence of ATc. HFFs were washed with HBSS (Gibco-BRL) at 2 h postinfection to remove extracellular parasites and 24 h later fixed for 20 min with 4% (wt/vol) paraformaldehyde in PBS. The number of parasites per vacuole was scored. Independent experiments were conducted three times, and 200 vacuoles were counted for each condition.

Fluorescence microscopy. For IFAs, intracellular tachyzoites grown on a monolayer of HFFs and incubated in the presence or absence of ATc for various periods of time were fixed for 20 min with 4% (wt/vol) paraformaldehyde in PBS, permeabilized for 10 min with 0.3% Triton X-100 in PBS, and blocked with 0.1% (wt/vol) BSA in PBS. The primary antibodies used for detection were anti-TgATRX1 (1/1,000), anti-mitochondrial F₁F₀ ATPase (1/1,000) (P. Bradley, unpublished data), anti-TgCPN60 (28) (1/2,000), anti-TgATG8 (26) (1/1,000), anti-AMA1 (56) (1/10,000), anti-TgIMC1 (36) (1/1,000), anti-GRA3 (55) (1/500), anti-RON4 (57) (1/500), and anti-centrin1 (1/500) (I. Cheeseman, unpublished data) antibodies. Staining of both nucleus and apicoplast DNAs was performed with fixed cells incubated for 5 min in a 1- μ g/ml DAPI solution. All images were acquired at the Montpellier RIO Imaging facility from a Zeiss Axio Imager Z2 epifluorescence microscope equipped with an ORCA-flash 4.0 camera (Hamamatsu) and driven by the ZEN software (Zeiss). Adjustments for brightness and contrast were applied uniformly to the entire image. For quantification, at least three independent replicates were used.

Imaging of live cells. Tachyzoites were inoculated onto confluent HFF monolayers grown in 35-mm glass bottom dishes (23-mm glass Fluorodish; WPI) and incubated at 37°C and 5% CO₂ in a humidified incubator for 16 to 24 h. Before imaging, the sample was transferred into a heated observation chamber (37°C) equilibrated with 5% CO₂. Imaging was carried out with a 100 \times 1.4 numerical aperture oil immersion objective (Nikon) mounted on an inverted microscope (Eclipse-Ti; Nikon) equipped with a CSU-W1 spinning-disc confocal head (Yokogawa). Two solid-state lasers were used as the excitation sources at 488 nm (100 mW) and 561 nm (100 mW) for GFP and Tomato RFP, respectively. Fluorescence emission was filtered with a trio dichroic mirror (Andor Technology) at 525/30 nm and 607/36 nm for GFP and RFP, respectively. Images were acquired with a Neo sCMOS camera (Andor Technology); the acquisition process was controlled by Andor iQ3 software (Andor Technology). Images were collected every 10 min; postacquisition processing was performed in ImageJ.

Structured-illumination microscopy. Sterile round coverslips were seeded to confluence with host HFFs. GFP-TgATG8 parasites were applied to the host cells and incubated for 40 h. The medium was removed, and the coverslips were then incubated with warm PBS (pH 7.4) for 10 min. Cells were fixed in 100% ice-cold methanol for 5 min, washed thrice with PBS for 5 min, and then blocked with PBS with 3% (wt/vol) BSA for 30 min. The primary antibodies used were anti-TgATRX1 (Bradley, unpublished) (1/300) and anti-TgCPN60 (28) (1/300) antibodies. Alexa Fluor 546- and Alexa Fluor 405-conjugated secondary antibodies were used at a dilution of 1/300. Superresolution microscopy was performed with a Zeiss ELYRA S1 (SR-SIM) microscope with a high-resolution Axio observer Z1 inverted microscope stand with transmitted

(HAL), UV (HBO) and high-power solid-state laser illumination sources (405/488/561 nm), a 100 \times oil immersion objective, and an Andor iXon EM-CCD camera. Images were acquired with ZEN software (Zeiss) with a SIM analysis module and analyzed with ImageJ.

Electron microscopy. Infected HFF monolayers grown for 24 h in ATc were fixed for 4 h at room temperature with 2.5% glutaraldehyde in 0.1 M cacodylate buffer (pH 7.4), washed with cacodylate buffer, and postfixed for 1 h in 1% osmium tetroxide in the same buffer, followed by 2 h in 2% uranyl acetate in water. Dehydration was performed with an ethanol series, and samples were impregnated with epon 118-ethanol (50:50) and then 100% epon 118. Polymerization was performed at 60°C for 48 h. Ultrathin 70-nm sections were cut with a Leica Ultracut Ultramicrotome, counterstained with uranyl acetate and lead citrate, and observed in a JEOL 1200 EXII transmission electron microscope. All chemicals were from Electron Microscopy Sciences, and solvents were from Sigma.

SUPPLEMENTAL MATERIAL

Supplemental material for this article may be found at <http://mbio.asm.org/lookup/suppl/doi:10.1128/mBio.01446-15/-/DCSupplemental>.

Table S1, DOCX file, 0.01 MB.
Figure S1, TIF file, 0.04 MB.
Figure S2, TIF file, 0.1 MB.
Figure S3, TIF file, 0.1 MB.
Figure S4, TIF file, 0.2 MB.
Figure S5, TIF file, 0.6 MB.
Figure S6, PDF file, 0.3 MB.
Figure S7, TIF file, 0.1 MB.
Movie S1, AVI file, 3.6 MB.
Movie S2, AVI file, 0.7 MB.

ACKNOWLEDGMENTS

We thank I. Cheeseman, P. Bradley, C. Beckers, L. Sheiner, W. Daher, D. Roos, and J. F. Dubremetz for their generous gifts of cell lines and antibodies. Thanks to the Montpellier RIO Imaging platform for access to their facility.

This work was supported by grant ANR-13-JSV3-0003 from the Agence Nationale de la Recherche to S.B. M.F.L. is a Ph.D. fellow from the Labex EpiGenMed. This work was also made possible through support from the CNRS, the Fondation pour la Recherche Médicale (Equipe FRM DEQ20130326508), and the Labex Parafra (ANR-11-LABX-0024). Further support was received from the National Institutes of Health through grant RO1AI 64671 to B.S. and a postdoctoral fellowship (T32AI060546) to M.J.C.; B.S. is a GRA distinguished investigator.

REFERENCES

- White NJ, Pukrittayakamee S, Hien TT, Faiz MA, Mokuolu OA, Don-dorp AM. 2014. Malaria. *Lancet* 383:723–735. [http://dx.doi.org/10.1016/S0140-6736\(13\)60024-0](http://dx.doi.org/10.1016/S0140-6736(13)60024-0).
- Montoya J, Liesenfeld O. 2004. Toxoplasmosis. *Lancet* 363:1965–1976. [http://dx.doi.org/10.1016/S0140-6736\(04\)16412-X](http://dx.doi.org/10.1016/S0140-6736(04)16412-X).
- Black MW, Boothroyd JC. 2000. Lytic cycle of *Toxoplasma gondii*. *Microbiol Mol Biol Rev* 64:607–623. <http://dx.doi.org/10.1128/MMBR.64.3.607-623.2000>.
- Francia ME, Striepen B. 2014. Cell division in apicomplexan parasites. *Nat Rev Microbiol* 12:125–136. <http://dx.doi.org/10.1038/nrmicro3184>.
- Sheffield HG, Melton ML. 1968. The fine structure and reproduction of *Toxoplasma gondii*. *J Parasitol* 54:209–226. <http://dx.doi.org/10.2307/3276925>.
- Nishi M, Hu K, Murray JM, Roos DS. 2008. Organellar dynamics during the cell cycle of *Toxoplasma gondii*. *J Cell Sci* 121:1559–1568. <http://dx.doi.org/10.1242/jcs.021089>.
- Hu K, Mann T, Striepen B, Beckers CJM, Roos DS, Murray JM. 2002. Daughter cell assembly in the protozoan parasite *Toxoplasma gondii*. *Mol Biol Cell* 13:593–606. <http://dx.doi.org/10.1091/mbc.01-06-0309>.
- van Dooren GG, Striepen B. 2013. The algal past and parasite present of the apicoplast. *Annu Rev Microbiol* 67:271–289. <http://dx.doi.org/10.1146/annurev-micro-092412-155741>.
- Sheiner L, Vaidya AB, McFadden GI. 2013. The metabolic roles of the

- endosymbiotic organelles of *Toxoplasma* and *Plasmodium* spp. *Curr Opin Microbiol* 16:452–458. <http://dx.doi.org/10.1016/j.mib.2013.07.003>.
10. Striepen B, Crawford MJ, Shaw MK, Tilney LG, Seeber F, Roos DS. 2000. The plastid of *Toxoplasma gondii* is divided by association with the centrosomes. *J Cell Biol* 151:1423–1434. <http://dx.doi.org/10.1083/jcb.151.7.1423>.
 11. Vaishnav S, Morrison DP, Gaji RY, Murray JM, Entzeroth R, Howe DK, Striepen B. 2005. Plastid segregation and cell division in the apicomplexan parasite *Sarcocystis neurona*. *J Cell Sci* 118:3397–3407. <http://dx.doi.org/10.1242/jcs.02458>.
 12. van Dooren GG, Reiff SB, Tomova C, Meissner M, Humbel BM, Striepen B. 2009. A novel dynamin-related protein has been recruited for apicoplast fission in *Toxoplasma gondii*. *Curr Biol* 19:267–276. <http://dx.doi.org/10.1016/j.cub.2008.12.048>.
 13. Feng Y, He D, Yao Z, Klionsky DJ. 2014. The machinery of macroautophagy. *Cell Res* 24:24–41. <http://dx.doi.org/10.1038/cr.2013.168>.
 14. Mizushima N, Levine B, Cuervo AM, Klionsky DJ. 2008. Autophagy fights disease through cellular self-digestion. *Nature* 451:1069–1075. <http://dx.doi.org/10.1038/nature06639>.
 15. Nakatogawa H, Ichimura Y, Ohsumi Y. 2007. Atg8, a ubiquitin-like protein required for autophagosome formation, mediates membrane tethering and hemifusion. *Cell* 130:165–178. <http://dx.doi.org/10.1016/j.cell.2007.05.021>.
 16. Shibutani ST, Yoshimori T. 2014. A current perspective of autophagosome biogenesis. *Cell Res* 24:58–68. <http://dx.doi.org/10.1038/cr.2013.159>.
 17. Brennand A, Gualdrón-López M, Coppens I, Rigden DJ, Ginger ML, Michels PAM. 2011. Autophagy in parasitic protists: unique features and drug targets. *Mol Biochem Parasitol* 177:83–99. <http://dx.doi.org/10.1016/j.molbiopara.2011.02.003>.
 18. Besteiro S, Brooks CF, Striepen B, Dubremetz J. 2011. Autophagy protein Atg3 is essential for maintaining mitochondrial integrity and for normal intracellular development of *Toxoplasma gondii* tachyzoites. *PLoS Pathog* 7:e1002416. <http://dx.doi.org/10.1371/journal.ppat.1002416>.
 19. Ghosh D, Walton JL, Roepe PD, Sinai AP. 2012. Autophagy is a cell death mechanism in *Toxoplasma gondii*. *Cell Microbiol* 14:589–607. <http://dx.doi.org/10.1111/j.1462-5822.2011.01745.x>.
 20. Tomlins AM, Ben-Rached F, Williams RA, Proto WR, Coppens I, Ruch U, Gilberger TW, Coombs GH, Mottram JC, Müller S, Langsley G. 2013. *Plasmodium falciparum* ATG8 implicated in both autophagy and apicoplast formation. *Autophagy* 9:1540–1552. <http://dx.doi.org/10.4161/aut.25832>.
 21. Cervantes S, Bunnik EM, Saraf A, Conner CM, Escalante A, Sardiú ME, Ponts N, Prudhomme J, Florens L, Le Roch KG. 2014. The multifunctional autophagy pathway in the human malaria parasite, *Plasmodium falciparum*. *Autophagy* 10:80–92. <http://dx.doi.org/10.4161/aut.26743>.
 22. Eickel N, Kaiser G, Prado M, Burda P, Roelli M, Stanway RR, Heussler VT. 2013. Features of autophagic cell death in *Plasmodium* liver-stage parasites. *Autophagy* 9:568–580. <http://dx.doi.org/10.4161/aut.23689>.
 23. Jayabalasingham B, Voss C, Ehrenman K, Romano JD, Smith ME, Fidock DA, Bosch J, Coppens I. 2014. Characterization of the ATG8-conjugation system in 2 *Plasmodium* species with special focus on the liver stage: possible linkage between the apicoplast and autophagy systems? *Autophagy* 10:269–284. <http://dx.doi.org/10.4161/aut.27166>.
 24. Kitamura K, Kishi-Itakura C, Tsuboi T, Sato S, Kita K, Ohta N, Mizushima N. 2012. Autophagy-related Atg8 localizes to the apicoplast of the human malaria parasite *Plasmodium falciparum*. *PLoS One* 7:e42977. <http://dx.doi.org/10.1371/journal.pone.0042977>.
 25. Navale R, Atul, Allanki AD, Sijwali PS. 2014. Characterization of the autophagy marker protein Atg8 reveals atypical features of autophagy in *Plasmodium falciparum*. *PLoS One* 9:e113220. <http://dx.doi.org/10.1371/journal.pone.0113220>.
 26. Kong-Hap MA, Mouammine A, Daher W, Berry L, Lebrun M, Dubremetz J, Besteiro S. 2013. Regulation of ATG8 membrane association by ATG4 in the parasitic protist *Toxoplasma gondii*. *Autophagy* 9:1334–1348. <http://dx.doi.org/10.4161/aut.25189>.
 27. Lavine MD, Arrizabalaga G. 2012. Analysis of monensin sensitivity in *Toxoplasma gondii* reveals autophagy as a mechanism for drug induced death. *PLoS One* 7:e42107. <http://dx.doi.org/10.1371/journal.pone.0042107>.
 28. Agrawal S, van Dooren GG, Beatty WL, Striepen B. 2009. Genetic evidence that an endosymbiont-derived endoplasmic reticulum-associated protein degradation (ERAD) system functions in import of apicoplast proteins. *J Biol Chem* 284:33683–33691. <http://dx.doi.org/10.1074/jbc.M109.044024>.
 29. DeRocher AE, Coppens I, Karnataka A, Gilbert LA, Rome ME, Feagin JE, Bradley PJ, Parsons M. 2008. A thioredoxin family protein of the apicoplast periphery identifies abundant candidate transport vesicles in *Toxoplasma gondii*. *Eukaryot Cell* 7:1518–1529. <http://dx.doi.org/10.1128/EC.00081-08>.
 30. Meissner M, Brecht S, Bujard H, Soldati D. 2001. Modulation of myosin A expression by a newly established tetracycline repressor-based inducible system in *Toxoplasma gondii*. *Nucleic Acids Res* 29:E115. <http://dx.doi.org/10.1093/nar/29.22.e115>.
 31. Fox BA, Ristuccia JG, Gigley JP, Bzik DJ. 2009. Efficient gene replacements in *Toxoplasma gondii* strains deficient for nonhomologous end joining. *Eukaryot Cell* 8:520–529. <http://dx.doi.org/10.1128/EC.00357-08>.
 32. Sheiner L, Demerly JL, Poulsen N, Beatty WL, Lucas O, Behnke MS, White MW, Striepen B. 2011. A systematic screen to discover and analyze apicoplast proteins identifies a conserved and essential protein import factor. *PLoS Pathog* 7. <http://dx.doi.org/10.1371/journal.ppat.1002392>.
 33. Pfefferkorn ER, Nothnagel RF, Borotz SE. 1992. Parasitocidal effect of clindamycin on *Toxoplasma gondii* grown in cultured cells and selection of a drug-resistant mutant. *Antimicrob Agents Chemother* 36:1091–1096. <http://dx.doi.org/10.1128/AAC.36.5.1091>.
 34. Fichera ME, Roos DS. 1997. A plastid organelle as a drug target in apicomplexan parasites. *Nature* 390:407–409. <http://dx.doi.org/10.1038/37132>.
 35. He CY, Shaw MK, Pletcher CH, Striepen B, Tilney LG, Roos DS. 2001. A plastid segregation defect in the protozoan parasite *Toxoplasma gondii*. *EMBO J* 20:330–339. <http://dx.doi.org/10.1093/emboj/20.3.330>.
 36. Mann T, Beckers C. 2001. Characterization of the subpellicular network, a filamentous membrane skeletal component in the parasite *Toxoplasma gondii*. *Mol Biochem Parasitol* 115:257–268. [http://dx.doi.org/10.1016/S0166-6851\(01\)00289-4](http://dx.doi.org/10.1016/S0166-6851(01)00289-4).
 37. Hartmann J, Hu K, He CY, Pelletier L, Roos DS, Warren G. 2006. Golgi and centrosome cycles in *Toxoplasma gondii*. *Mol Biochem Parasitol* 145:125–127. <http://dx.doi.org/10.1016/j.molbiopara.2005.09.015>.
 38. Behnke MS, Wootton JC, Lehmann MM, Radke JB, Lucas O, Nawas J, Sibley LD, White MW. 2010. Coordinated progression through two sub-transcriptomes underlies the tachyzoite cycle of *Toxoplasma gondii*. *PLoS One* 5:e12354. <http://dx.doi.org/10.1371/journal.pone.0012354>.
 39. Slobodkin MR, Elazar Z. 2013. The Atg8 family: multifunctional ubiquitin-like key regulators of autophagy. *Essays Biochem* 55:51–64. <http://dx.doi.org/10.1042/bse0550051>.
 40. Kimura S, Noda T, Yoshimori T. 2008. Dynein-dependent movement of autophagosomes mediates efficient encounters with lysosomes. *Cell Struct Funct* 33:109–122. <http://dx.doi.org/10.1247/csf.08005>.
 41. Fass E, Shvets E, Degani I, Hirschberg K, Elazar Z. 2006. Microtubules support production of starvation-induced autophagosomes but not their targeting and fusion with lysosomes. *J Biol Chem* 281:36303–36316. <http://dx.doi.org/10.1074/jbc.M607031200>.
 42. Mann SS, Hammarback JA. 1994. Molecular characterization of light chain 3. A microtubule binding subunit of MAP1A and MAP1B. *J Biol Chem* 269:11492–11497.
 43. Xie R, Nguyen S, McKeehan K, Wang F, McKeehan WL, Liu L. 2011. Microtubule-associated protein 1S (MAP1S) bridges autophagic components with microtubules and mitochondria to affect autophagosomal biogenesis and degradation. *J Biol Chem* 286:10367–10377. <http://dx.doi.org/10.1074/jbc.M110.206532>.
 44. Pampliega O, Orhon I, Patel B, Sridhar S, Díaz-Carretero A, Beau I, Codogno P, Satir BH, Satir P, Cuervo AM. 2013. Functional interaction between autophagy and ciliogenesis. *Nature* 502:194–200. <http://dx.doi.org/10.1038/nature12639>.
 45. Shaw MK, Compton HL, Roos DS, Tilney LG. 2000. Microtubules, but not actin filaments, drive daughter cell budding and cell division in *Toxoplasma gondii*. *J Cell Sci* 113:1241–1254.
 46. Noda NN, Ohsumi Y, Inagaki F. 2010. Atg8-family interacting motif crucial for selective autophagy. *FEBS Lett* 584:1379–1385. <http://dx.doi.org/10.1016/j.febslet.2010.01.018>.
 47. Wild P, McEwan DG, Dikic I. 2014. The LC3 interactome at a glance. *J Cell Sci* 127:3–9. <http://dx.doi.org/10.1242/jcs.140426>.
 48. Jacot D, Daher W, Soldati-Favre D. 2013. *Toxoplasma gondii* myosin F,

- an essential motor for centrosomes [sic] positioning and apicoplast inheritance. *EMBO J* 32:1702–1716. <http://dx.doi.org/10.1038/emboj.2013.113>.
49. Kong S, Wada M. 2014. Recent advances in understanding the molecular mechanism of chloroplast photorelocation movement. *Biochim Biophys Acta* 1837:522–530. <http://dx.doi.org/10.1016/j.bbabi.2013.12.004>.
 50. Morrissette NS, Sibley LD. 2002. Cytoskeleton of apicomplexan parasites. *Microbiol Mol Biol Rev* 66:21–38. <http://dx.doi.org/10.1128/MMBR.66.1.21-38.2002>.
 51. van Dooren GG, Marti M, Tonkin CJ, Stimmler LM, Cowman AF, McFadden GI. 2005. Development of the endoplasmic reticulum, mitochondrion and apicoplast during the asexual life cycle of *Plasmodium falciparum*: organelle dynamics in *Plasmodium falciparum*. *Mol Microbiol* 57:405–419. <http://dx.doi.org/10.1111/j.1365-2958.2005.04699.x>.
 52. Stanway RR, Mueller N, Zobiak B, Graewe S, Froehlke U, Zessin PJM, Aepfelbacher M, Heussler VT. 2011. Organelle segregation into Plasmodium liver stage merozoites: Plasmodium organelle segregation. *Cell Microbiol* 13:1768–1782. <http://dx.doi.org/10.1111/j.1462-5822.2011.01657.x>.
 53. Morlon-Guyot J, Berry L, Chen C, Gubbels M, Lebrun M, Daher W. 2014. The *Toxoplasma gondii* calcium-dependent protein kinase 7 is involved in early steps of parasite division and is crucial for parasite survival. *Cell Microbiol* 16:95–114. <http://dx.doi.org/10.1111/cmi.12186>.
 54. Couvreur G, Sadak A, Fortier B, Dubremetz JF. 1988. Surface antigens of *Toxoplasma gondii*. *Parasitology* 97:1–10. <http://dx.doi.org/10.1017/S0031182000066695>.
 55. Achbarou A, Mercereau-Puijalon O, Sadak A, Fortier B, Leriche MA, Camus D, Dubremetz JF. 1991. Differential targeting of dense granule proteins in the parasitophorous vacuole of *Toxoplasma gondii*. *Parasitology* 103:321–329. <http://dx.doi.org/10.1017/S0031182000059837>.
 56. Lamarque MH, Roques M, Kong-Hap M, Tonkin ML, Rugarabamu G, Marq J-B, Penarete-Vargas DM, Boulanger MJ, Soldati-Favre D, Lebrun M. 2014. Plasticity and redundancy among AMA-RON pairs ensure host cell entry of *Toxoplasma* parasites. *Nat Commun* 5:4098.
 57. Besteiro S, Michelin A, Poncet J, Dubremetz J, Lebrun M. 2009. Export of a *Toxoplasma gondii* rhoptry neck protein complex at the host cell membrane to form the moving junction during invasion. *PLoS Pathog* 5:e1000309. <http://dx.doi.org/10.1371/journal.ppat.1000309>.